Proline Peptide Bond Isomerization in Ubiquitin under Folding and Denaturing Conditions by Pressure-Jump NMR

Elahe Masoumzadeh, Jinfa Ying, James L. Baber, Philip Anfinrud and Ad Bax

Supporting Information

TEXT

***cis*-Pro signal in double pressure-jump experiment**

At the end of the high-pressure denaturation period, we assume the *cis* population has reached its equilibrium fractional value A (e.g. $A \approx 0.09$ for P19). During the subsequent low-pressure delay of duration T_{LP} (Fig. 4a), the *cis* fraction reduces to $A \exp(-k_{ct}T_{LP})$, where k_{ct} is the *cis* to *trans* isomerization rate at low pressure. Immediately following the next pressure jump back to high pressure, the time domain signal for the first t_1 increment (describing the *cis* fraction for *e.g.* S20) of the 2D SOFAST-HMQC spectrum ($t_1 = 0$) is written as:

$$I(t_1,T_{LP}) = A \exp(-k_{ct}T_{LP}) \exp(i\Omega_N t_1)\exp(-t_1/T_{2N}) \exp(i\Omega_H t_2) \exp(-t_2/T_{2H}) \quad (1)$$

where Ω_N and Ω_H are the angular ^{15}N and ^{1}H resonance offset frequencies, and T_{2N} and T_{2H} are the decay constants for transverse ^{15}N and ^{1}H magnetization of the *cis* isomer during the high-pressure readout. Without loss of generality, we simplify the analysis below by only considering the signal dependence on the duration of the evolution period, t_1:

$$I(t_1,T_{LP}) = A \exp(-k_{ct}T_{LP}) \exp(-t_1/T_{2N}) \quad (2)$$

Eq. 2 represents the signal of interest, from which k_{ct} is to be derived. However, after the second jump (back to high pressure; Fig. 4a), the *cis* fraction will slowly recover to its equilibrium value, A, at a rate given by k_{ex} where k_{ex} is the sum of the *cis*-to-*trans* and *trans*-to-*cis* isomerization rates at high pressure. Therefore, after jumping back to high pressure for detection, the *cis* fraction generally will contain an additional "high pressure recovery" component:

$$I_r(t_1) = A\ \{1- \exp(-k_{ct}T_{LP})\}\ [1 - \exp(-Nk_{ex}t_1)]\ \exp(-t_1/T_{2N}) \quad (3)$$

where $N = 2\times NS\times(d1+aq)/\Delta t_1$, with NS being the total number of scans collected per (complex) t_1 increment, Δt_1, aq the duration of the pulse sequence including its t_2 acquisition period, and d1 is the delay between consecutive scans in the high-pressure readout SOFAST-HMQC.

So, the t_1 time domain collected for a given low-pressure duration T_{LP} (sum of eqs 2 and 3) consists of five components:

$$I(t_1,T_{LP}) = A\ \exp(-k_{ct}T_{LP})\ \exp(-t_1/T_{2N}) \quad (4A)$$

$$I(t_1,T_{LP}) = -\ A\ \exp(-k_{ct}T_{LP})\ \exp(-t_1/T_{2N}) \quad (4B)$$

$$I(t_1,T_{LP}) = A\ \exp(-t_1/T_{2N}) \quad (4C)$$

$$I(t_1,T_{LP}) = A\ \exp(-k_{ct}T_{LP})\ \exp(-Nk_{ex}t_1)\ \exp(-t_1/T_{2N}) = A\ \exp(-k_{ct}T_{LP})\ \exp\{(-Nk_{ex}-R_2)\ t_1\} \quad (4D)$$

$$I(t_1,T_{LP}) = -A\ \exp(-Nk_{ex}t_1)\ \exp(-t_1/T_2)\ = -A\ \exp\{(-Nk_{ex}-R_2)\ t_1\} \quad (4E)$$

with $R_2 = 1/T_{2N}$.

where 4A and 4B cancel one another, leaving:

$$I(t_1,T_{LP}) = A\ \exp(-R_2\ t_1) \quad (5A)$$

$$I(t_1,T_{LP}) = A\ \{\exp(-k_{ct}T_{LP})\ -\ 1\}\ \exp\{(-Nk_{ex}-R_2)\ t_1\} \quad (5B)$$

As a result, for $T_{LP} = 0$, we obtain:

$$I(t_1,0) = A\ \exp(-R_2\ t_1) \quad (6A)$$

whereas for $T_{LP} \rightarrow \infty$:

$$I(t_1, \infty) = A\ [\exp(-R_2\ t_1) - \exp\{(-Nk_{ex}-R_2)\ t_1\}] \quad (6B)$$

Eq. 6B shows that the Fourier transform of $I(t_1, \infty)$ corresponds to the difference between two Lorentzians with ^{15}N linewidths determined by R_2 and by R_2+Nk_{ex}, respectively. The second

component causes a (small) offset in the decay profile of the *cis* isomer intensity of the double-jump experiment that needs to be accounted for, either by simulating its effect based on the known high-pressure k_{ex} value, or by using an adjustable offset parameter in the fit of the exponential decay of *cis* intensities for increasing T_{LP}.

Effect of pressure jump on sample temperature

To assess the time required for temperature stabilization after a pressure jump induced by the adiabatic compression/decompression of the aqueous solvent, we monitored the chemical shift of TSP (3-(trimethylsilyl)propionic-2,2,3,3-d4 acid sodium salt, trisodium phosphate) in a 99.9% D_2O/0.1% H_2O sample by monitoring the temperature-dependent ^{1}HDO chemical shift relative to TSP, which increases by 10.32 ppb/°C.[1]

A series of 1D spectra were acquired for 50 seconds following a jump from 1 bar to 2.4 kbar, and after temperature equilibration at high pressure, a similar set of 1D spectra was recorded immediately following a drop in pressure from 2.4 kbar to 1 bar. The chemical shift of HDO relative to TSP was recorded in each spectrum (Fig. S4). The plot of HDO chemical shift as a function of time revealed a rapid change during the initial 5 seconds, followed by a more gradual temperature change with the sample reaching its set temperature after *ca* 20 s.

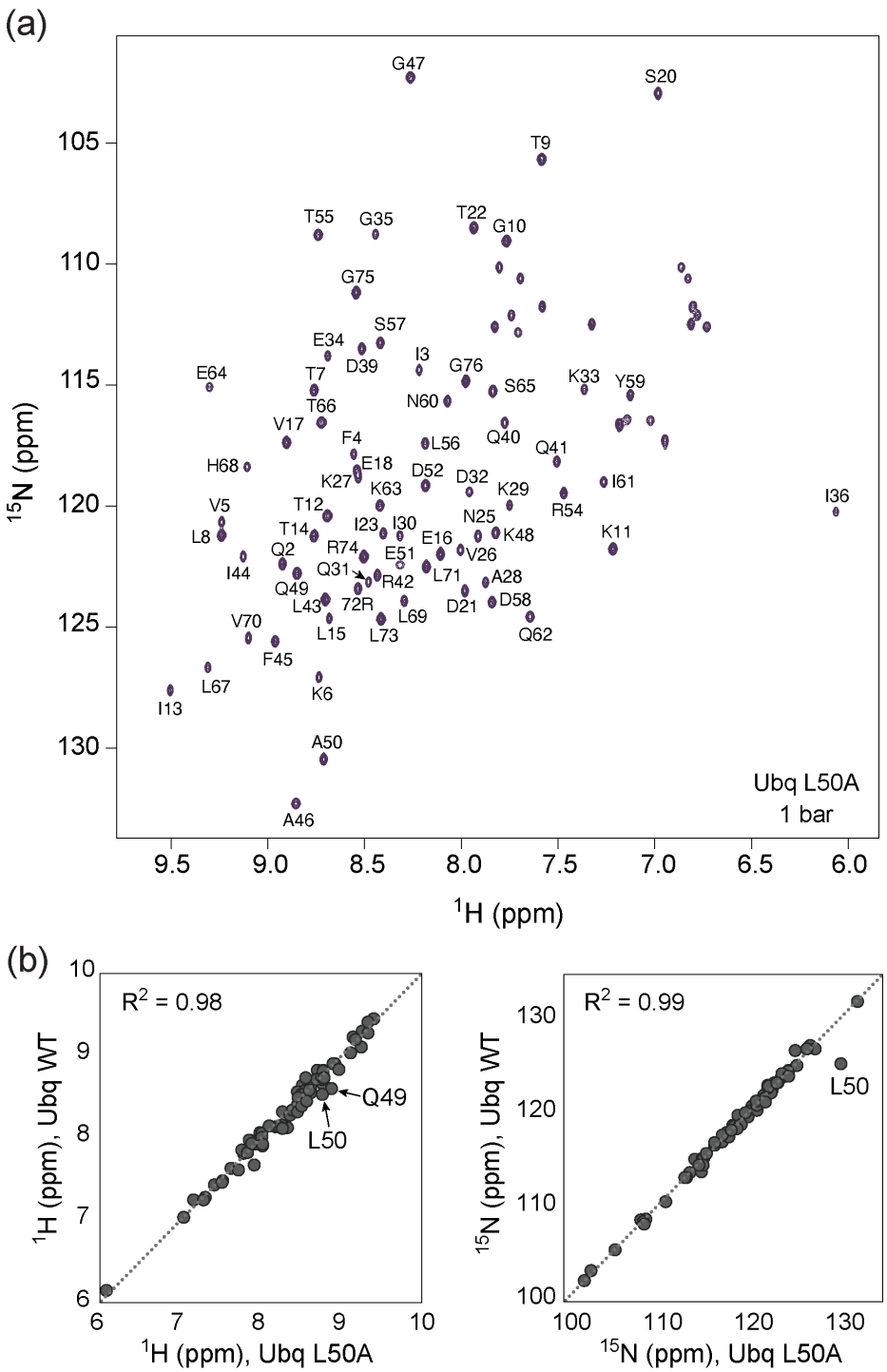

Figure S1. ^{1}H and ^{15}N chemical shift assignments of L50A ubiquitin, recorded at 278 K, 1 bar, 25 mM phosphate buffer pH 6.4 (at 1 bar). (a) 600 MHz ^{1}H -^{15}N HSQC NMR spectrum (b) ^{1}H and ^{15}N chemical shifts at 1 bar vs values observed for wild-type ubiquitin. Chemical shift values of L50A ubiquitin (folded, and unfolded at 1 bar, as well as unfolded at 2.4 kbar) are included in Table S1.

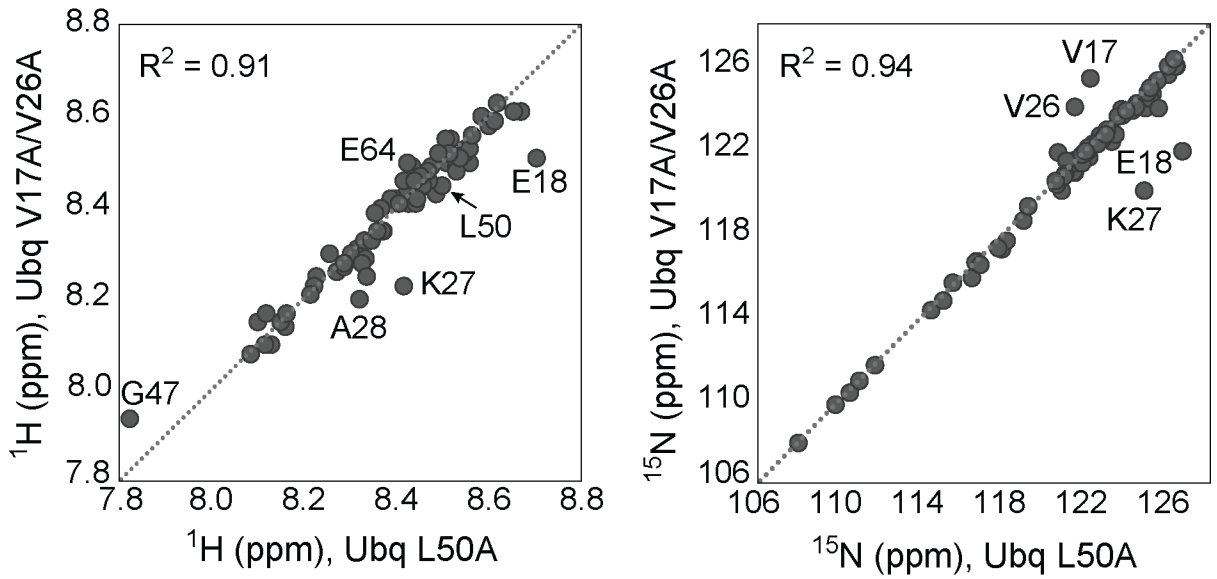

Figure S2. Comparison of ^{1}H and ^{15}N chemical shifts of pressure-denatured L50A ubiquitin with those of the V17A/V26A mutant, at 278 K, 25 mM phosphate buffer pH 6.4 (at 1 bar).

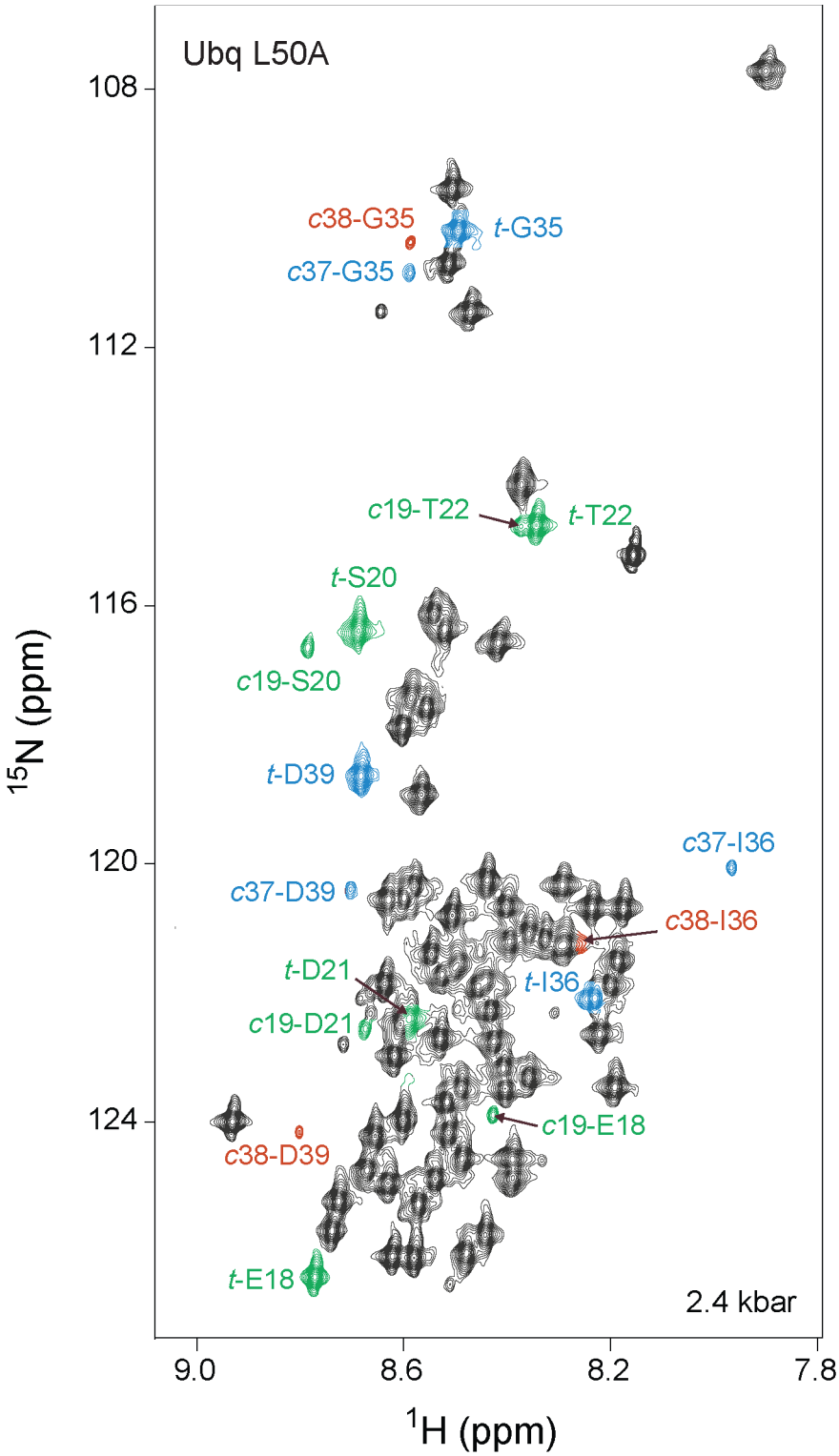

Figure S3. 800-MHz ^{1}H-^{15}N HSQC NMR spectrum of pressure-denatured L50A ubiquitin, recorded at 278 K, 2.4 kbar, 25 mM phosphate buffer pH 6.4 (at 1 bar). Resonances of the resolved *cis* isomer signals, together with those of their corresponding *trans* resonances, are marked.

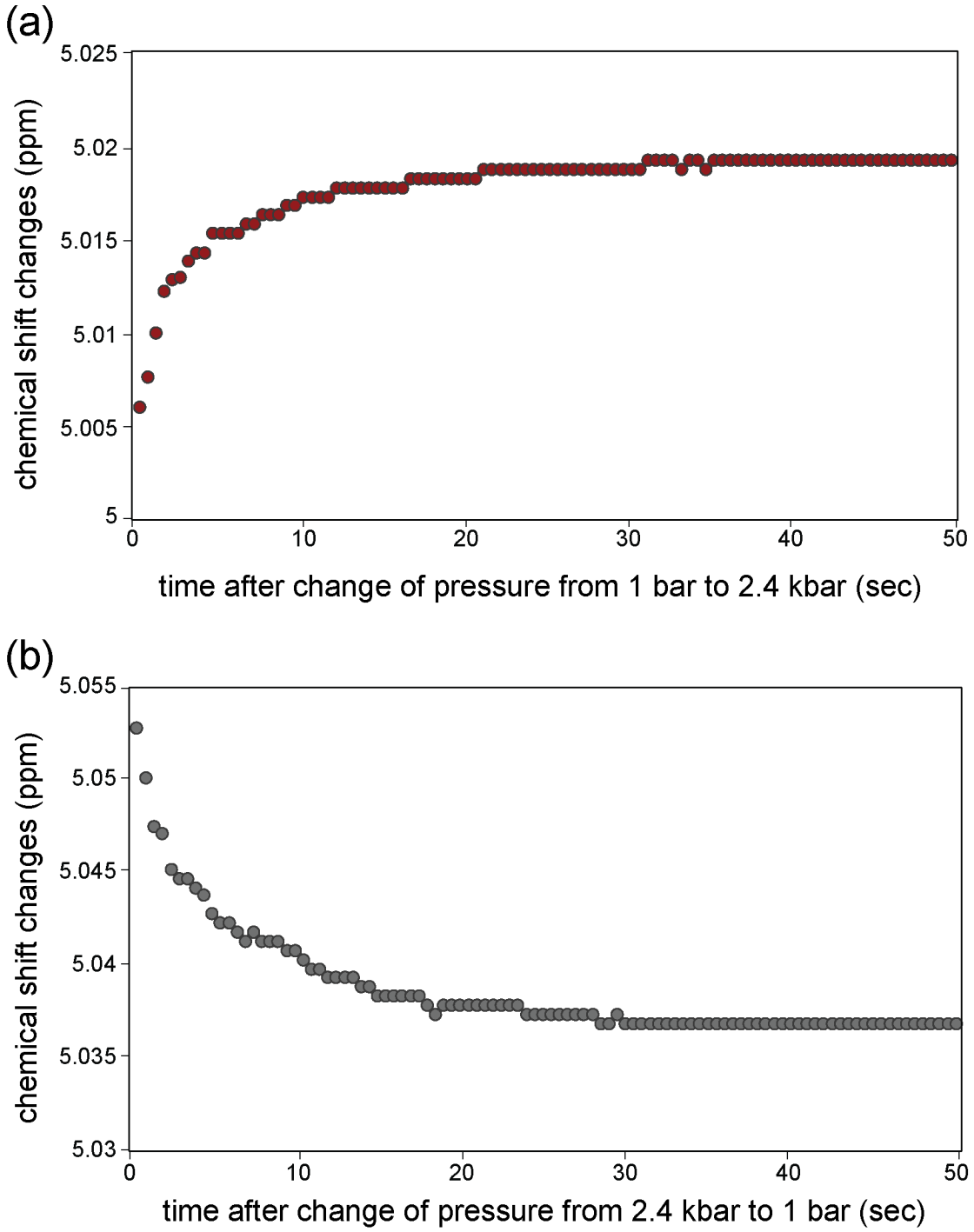

Figure S4. Chemical shift of HDO relative to trimethylsilylpropanoic acid (TSP), following a pressure jump (a) from 1 bar to 2.4 kbar, and (b) from 2.4 kbar to 1 bar, measured at pH 8.5, for a "set" temperature of 276 K. The graphs correspond to series of 1D spectra, taken at 0.5 s intervals, after switching the pressure, with the start of the first FID at 0.5 s after the pressure drop. The change in solvent temperature can be derived from the reported chemical shifts by using a HDO temperature coefficient of 10.32 ppb/°C.[1]

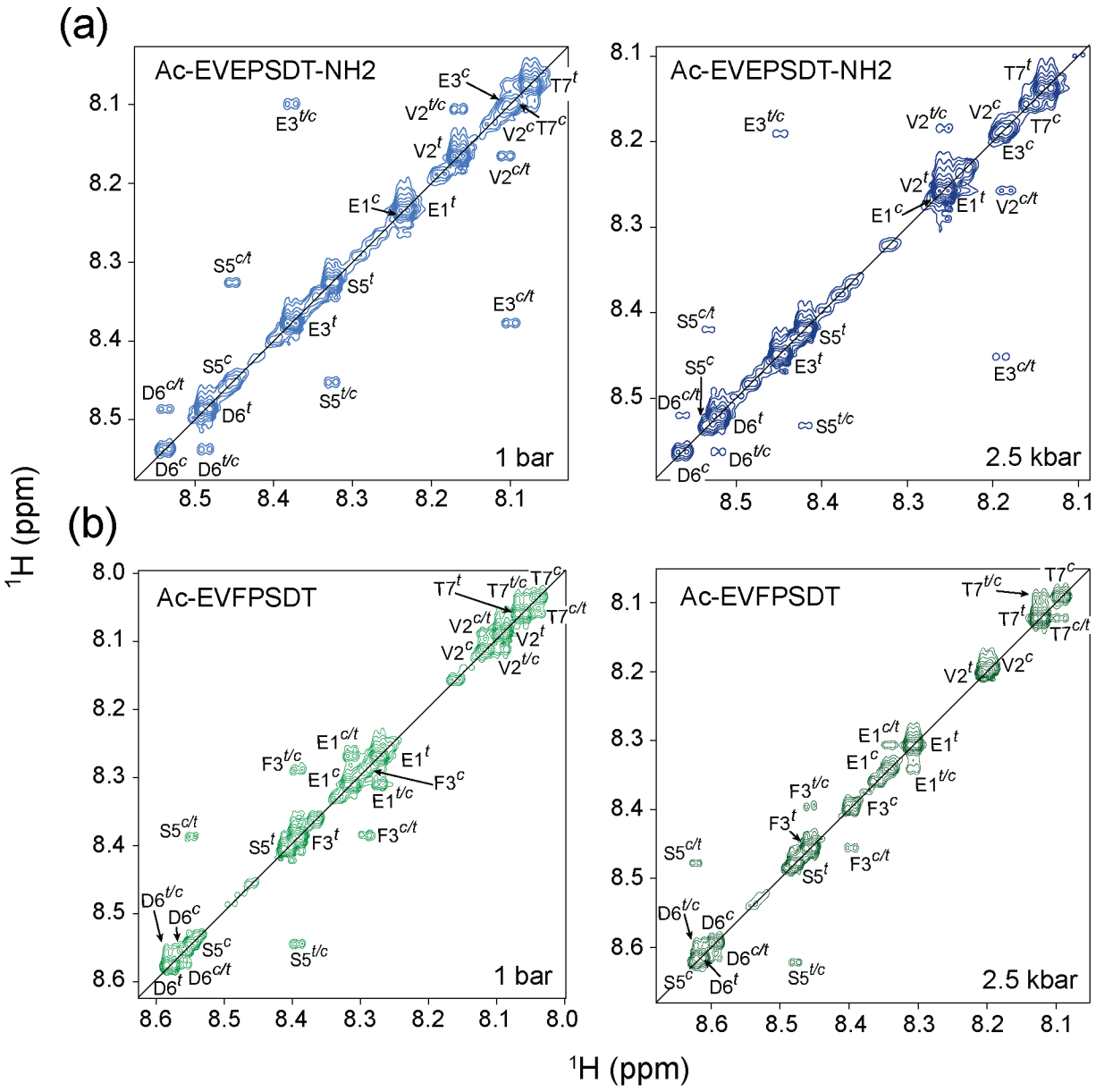

Figure S5. 700-MHz 2D exchange spectrum for the amide region of the heptapeptides (a) acetyl-EVEPSDT-NH_2 and (b) acetyl-EVFPSDT, both recorded at 1 bar (left panels) and 2.5 kbar (right panels), 327 K, pH 3.8, using a mixing time of 400 ms. The 2D spectrum was ^{1}H-^{1}H was decoupled in the F_1 (vertical) dimension by using a combination of a non-selective 180° and an amide-selective REBURP 180° pulse [2]. Isomerization rates, k_{ex}, were calculated based on the intensities of the well resolved cross- and diagonal-peak intensities of residues (a) V2, E3, S5 and D6, and (b) E1, V2, S5 and T7, using eq S12 described of Miloushev *et al.*[3]. Individual k_{ct} and k_{tc} rate constants were derived from k_{ex} by measurement of the equilibrium *cis* and *trans* populations, obtained from HSQC spectra recorded at both 1 bar and 2.5 kbar of pressure, that yielded statistically indistinguishable values at the two pressures of (a) 9.6 ± 0.8 % and (b) 18.9 ± 1.2 %. For isomerization rates at various temperatures, and derived activation energies, see Table S2.

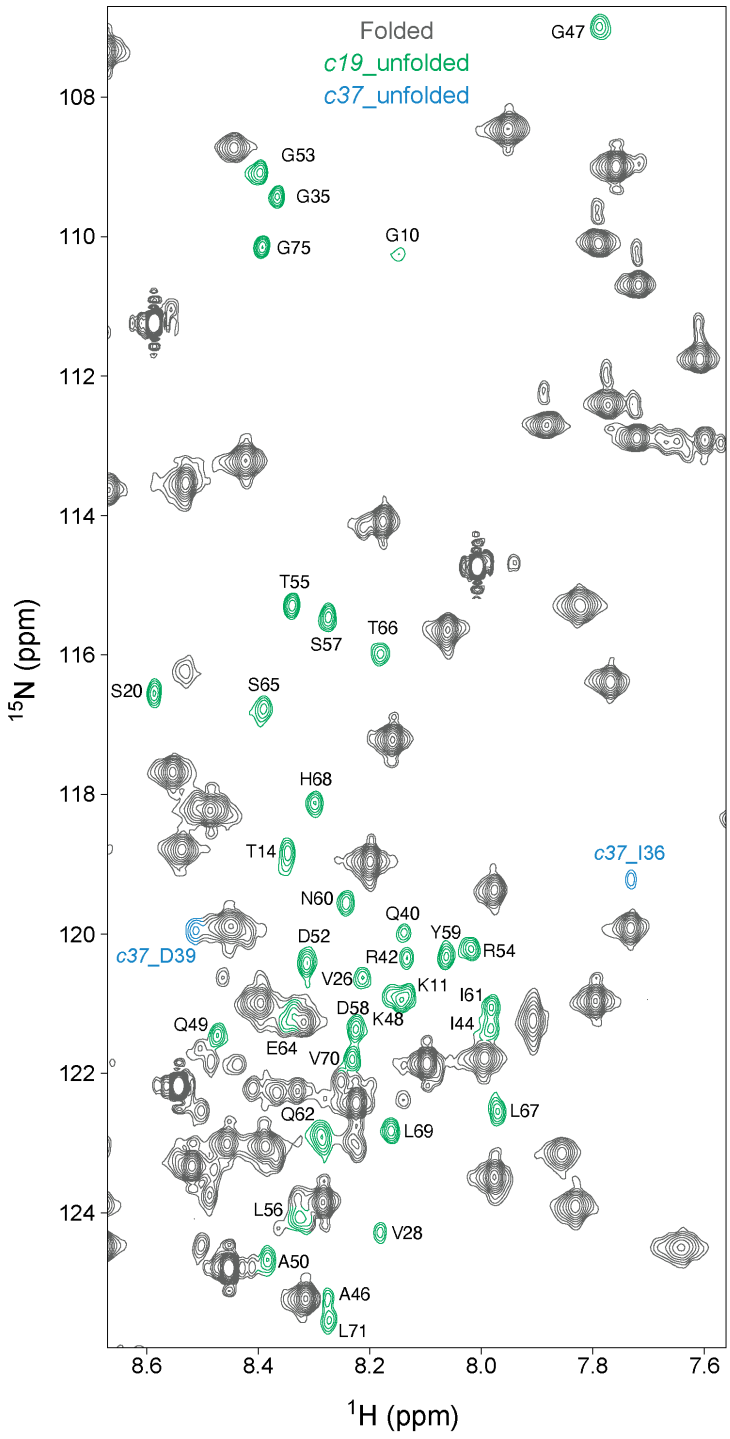

Figure S6. Region of a 10-minute 800-MHz HSQC spectrum containing weak, near random-coil signals of L50A ubiquitin, started 4 minutes after first dropping the pressure from 2.4 kbar to 1 bar at 277 K, followed by slowly lowering the temperature to 267.9 K during the 4 minutes after the pressure drop. Resonances corresponding to *cis*-P19 are shown in green, and those for *cis*-P37 in blue. No signals corresponding to *cis*-P38 remain visible at this time point.

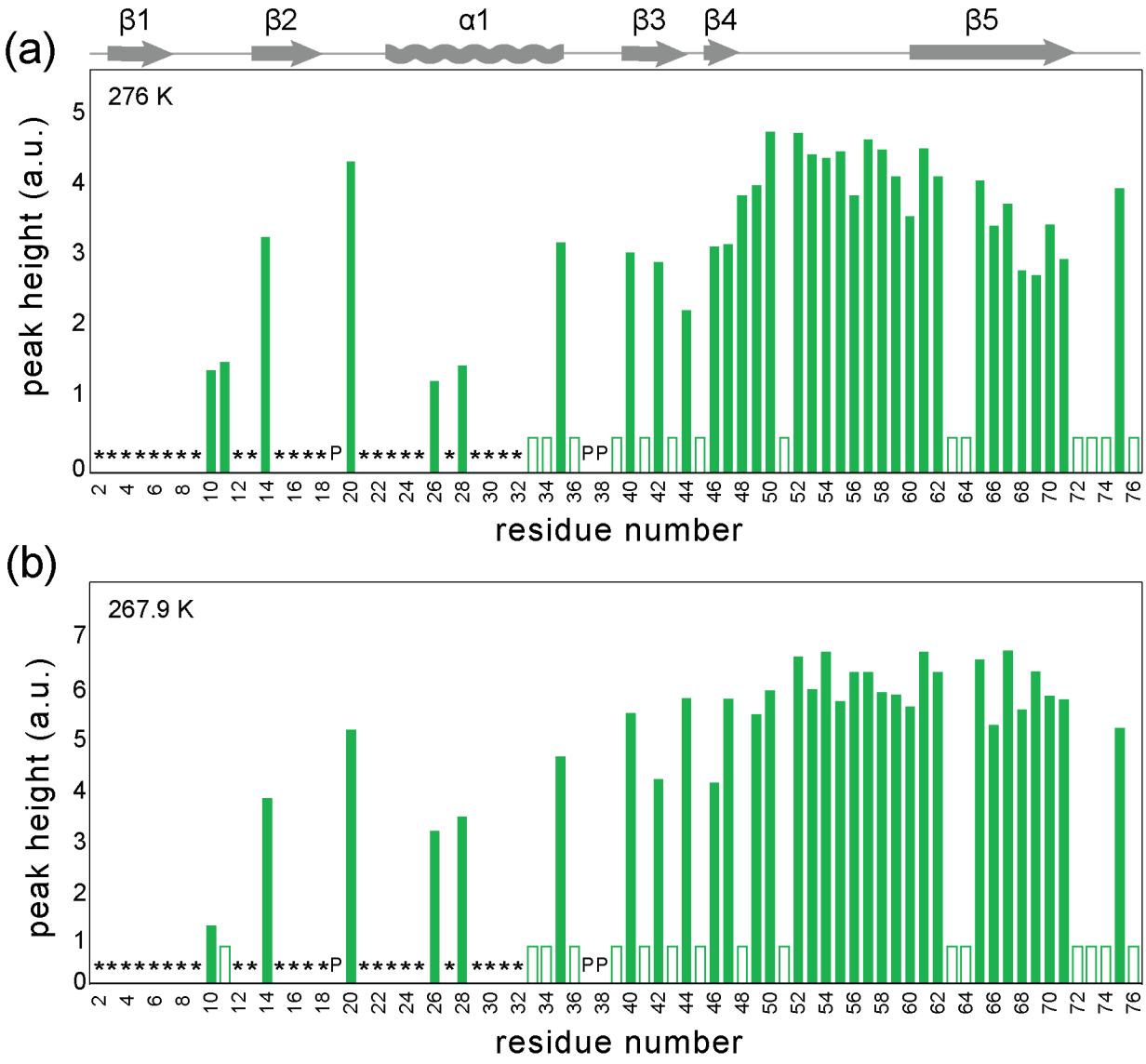

Figure S7. Intensities of amide ^{1}H-^{15}N correlation as a function of residue for weak signals with near random coil chemical shifts that remain visible shortly after dropping the pressure from 2.4 kbar to 1 bar. (a) SOFAST-HMQC intensities at 3 minutes (HMQC-midpoint) after the pressure drop at 276 K (from Fig. S8). (b) HSQC intensities at 9 minutes (HSQC-midpoint) at 267.9 K (from Fig. S6). Intensities that could not be measured due to (partial) overlap with nearby signals from natively folded protein are displayed as low open bars. The absence of near-random-coil unfolded amide signals is indicated with asterisks.

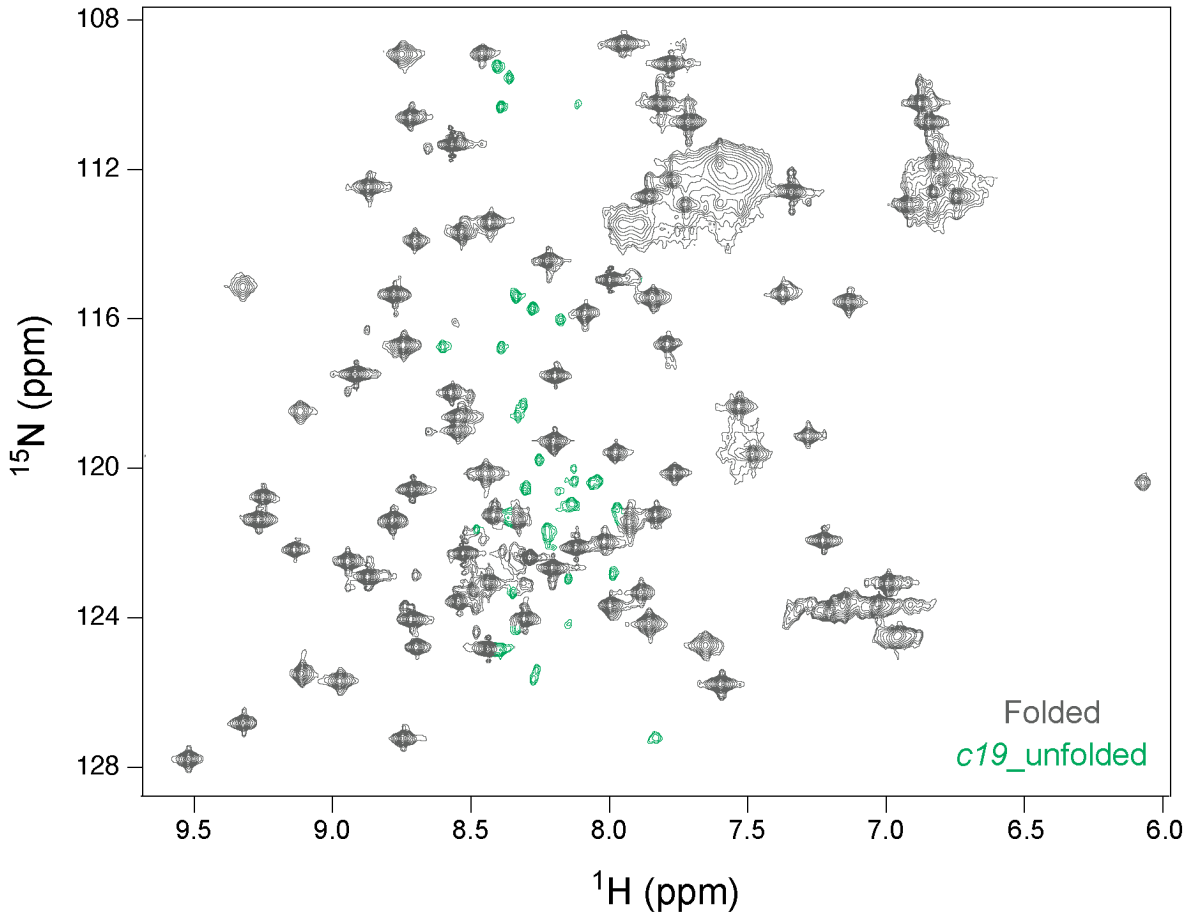

Figure S8. 900-MHz SOFAST-HMQC spectrum (3 min recording time) of L50A ubiquitin, started 1 minute after dropping the pressure from 2.4 kbar to 1 bar at 276K. Resonances from unfolded species (shown in green) correspond to *cis*-P19 (see also Fig. S6).

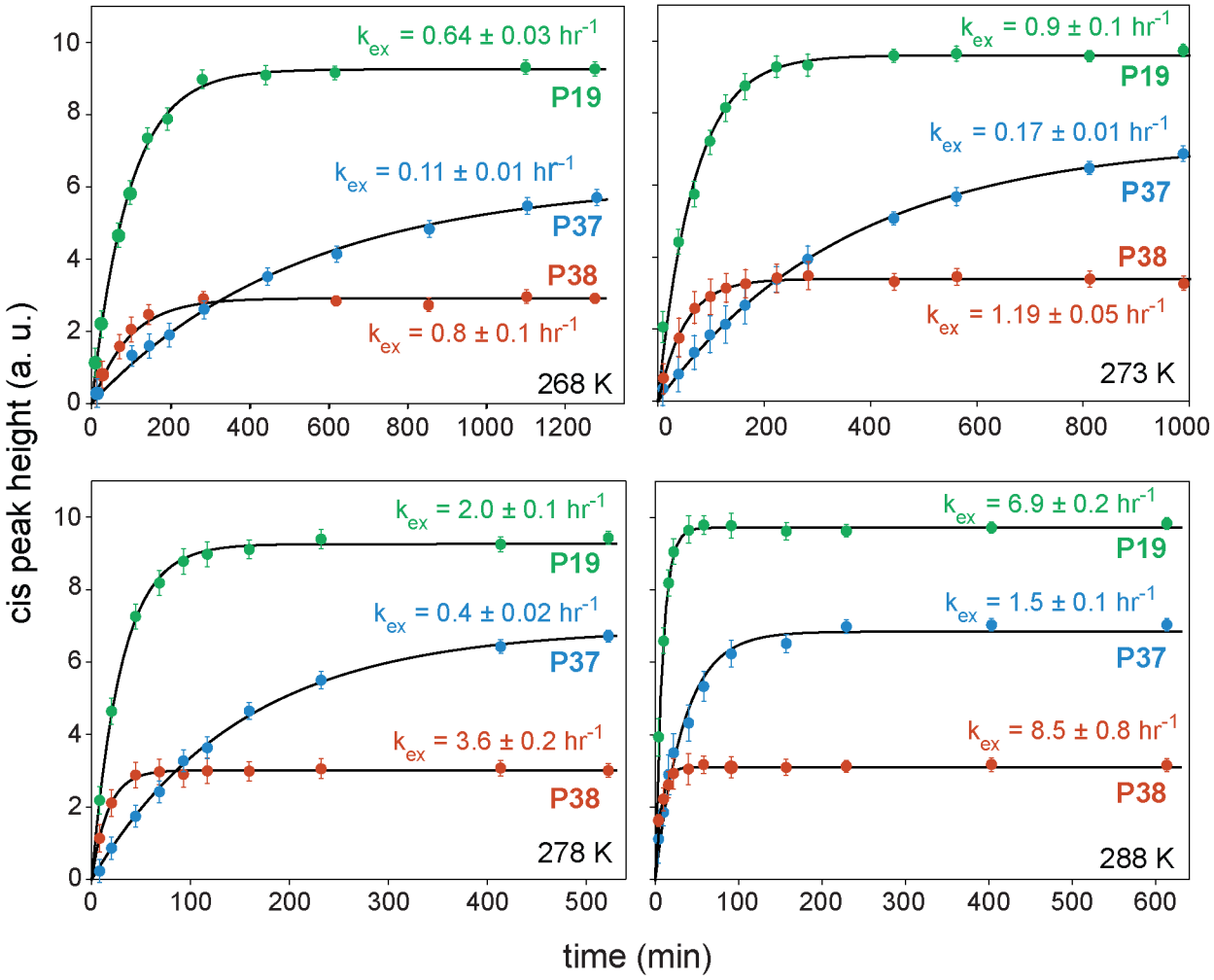

Figure S9. Growth of resonance intensity for signals of pressure-denatured L50A ubiquitin after a pressure jump to 2.4 kbar that correspond to *cis* isomers for P19 (green), P37 (blue) and P38 (red) at 268K, 273K, 278K and 288K.

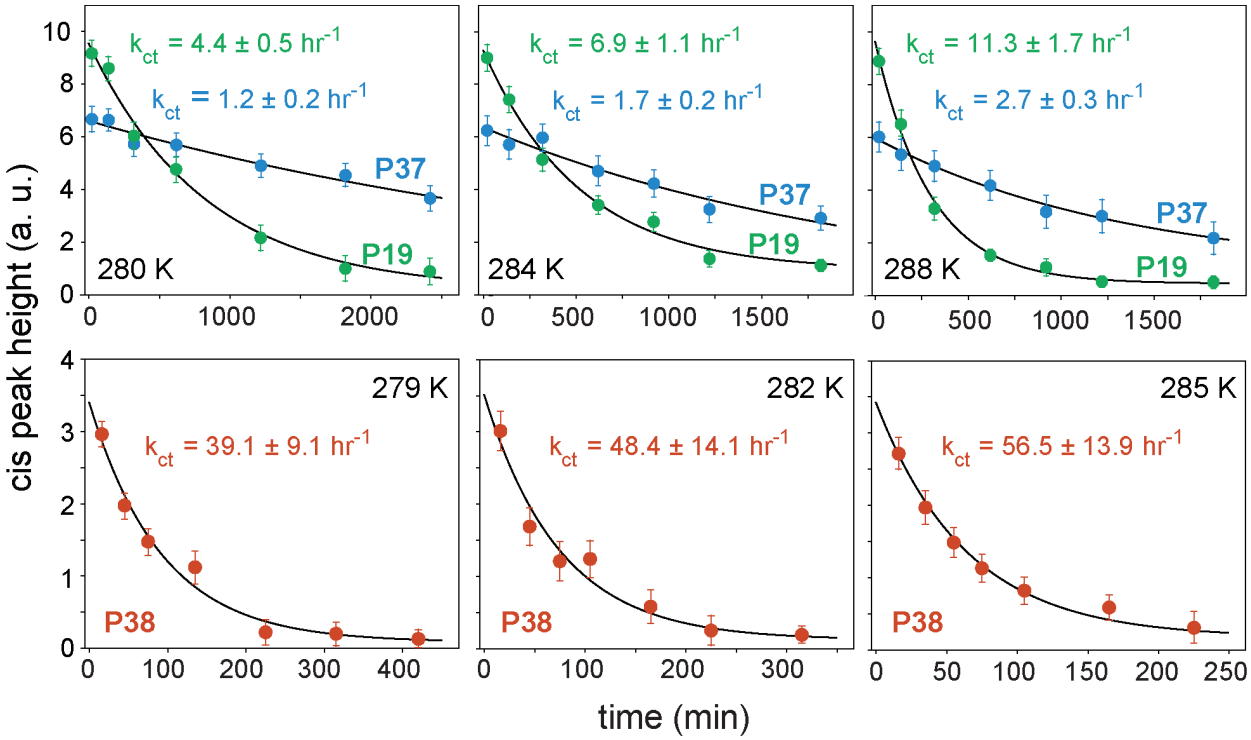

Figure S10. Mono-exponential decay fits for the intensities of D21 (green: *cis*-P19) and I36 (blue: *cis*-P37) at 280 K, 284 K, and 288 K (top row), and D39 (red: *cis*-P38) at 279 K, 282 K and 285 K (bottom row) obtained from double pressure-jump NMR experiments (see Figure 4).

Table S1. ^{1}H and ^{15}N chemical shifts of folded L50A ubiquitin at 278 K, 1 bar, 25 mM phosphate buffer pH 6.4 (at 1 bar), and in the unfolded state at 1 bar (obtained from extrapolation of the pressure-dependent values) and 2.4 kbar.

	folded (1bar)		unfolded (1bar)		unfolded (2.4kbar)	
residue	HN	N	HN	N	HN	N
2	8.92	122.34	8.60	123.95	8.95	123.93
3	8.21	114.35	8.71	123.32	8.62	123.93
4	8.55	117.91	8.54	125.18	8.76	125.65
5	9.22	120.64	8.62	123.91	8.40	124.56
6	8.76	127.17	8.57	125.75	8.60	126.06
7	8.75	115.22	8.78	117.10	8.57	117.53
8	9.23	121.13	8.23	124.54	8.74	125.18
9	7.58	105.67	8.46	112.86	8.39	114.09
10	7.77	109.07	8.21	111.08	8.49	111.39
11	7.21	121.76	8.62	121.22	8.32	121.21
12	8.68	120.40	8.75	118.15	8.62	117.82
13	9.51	127.57	8.55	125.01	8.65	124.91
14	8.75	121.13	8.69	119.99	8.62	120.51
15	8.68	124.66	8.61	126.08	8.64	126.03
16	8.10	121.99	8.50	122.80	8.64	122.92
17	8.90	117.38	8.81	121.92	8.47	121.86
18	8.54	118.55	8.63	126.70	8.79	126.36
20	6.98	102.92	8.57	115.86	8.71	116.34
21	7.98	123.52	8.36	122.65	8.61	122.34
22	7.93	108.49	8.42	114.68	8.36	114.70
23	8.40	121.12	8.67	123.49	8.42	123.44
24			8.61	124.28	8.67	124.17
25	7.91	121.29	8.34	120.52	8.65	120.51
26	8.00	121.84	8.52	121.35	8.34	121.13
27	8.53	118.77	8.38	124.70	8.50	124.53
28	7.86	123.14	8.42	124.86	8.41	124.83
29	7.75	119.97	8.44	121.21	8.41	121.15
30	8.31	121.24	8.70	123.45	8.42	123.13
31	8.47	123.13	8.60	125.07	8.69	124.70
32	7.95	119.41	8.62	122.71	8.62	122.44
33	7.36	115.19	8.61	121.97	8.51	121.58
34	8.69	113.81	8.55	121.50	8.56	121.35
35	8.44	108.77	8.26	109.91	8.51	110.13
36	6.06	120.24	8.67	122.53	8.25	122.02

39	8.50	113.49	8.37	118.74	8.70	118.59
40	7.77	116.55	8.44	120.41	8.31	120.28
41	7.50	118.17	8.35	120.65	8.42	120.61
42	8.42	122.90	8.25	121.08	8.37	121.04
43	8.69	123.87	8.19	122.70	8.24	122.58
44	9.15	122.15	8.54	121.93	8.22	121.84
45	8.95	125.45	8.48	124.57	8.53	124.11
46	8.89	132.38	7.97	126.13	8.46	125.69
47	8.25	102.25	8.35	107.55	7.91	107.64
48	7.81	121.13	8.70	121.27	8.30	121.19
49	8.85	122.85	8.61	122.18	8.65	121.79
50	8.71	130.47	8.66	125.40	8.59	125.21
51	8.31	122.42	8.51	120.48	8.59	120.29
52	8.18	119.15	8.59	121.02	8.52	120.74
53			8.24	109.57	8.52	109.47
54	7.47	119.46	8.53	120.60	8.19	120.63
55	8.74	108.80	8.54	115.91	8.56	116.07
56	8.18	117.40	8.48	124.79	8.55	124.81
57	8.41	113.24	8.42	116.20	8.54	116.29
58	7.84	123.99	8.25	121.96	8.46	121.75
59	7.12	115.42	8.45	120.71	8.25	120.62
60	8.07	115.65	8.16	120.23	8.45	120.19
61	7.26	119.02	8.54	121.41	8.20	121.46
62	7.64	124.57	8.49	123.76	8.50	123.41
63	8.41	119.98	8.53	122.88	8.44	122.70
64	9.30	115.10	8.61	121.65	8.51	121.50
65	7.83	115.24	8.39	117.20	8.60	117.38
66	8.71	116.60	8.20	116.40	8.43	116.53
67	9.30	126.74	8.56	123.43	8.21	123.39
68	9.10	118.69	8.37	119.03	8.58	118.86
69	8.27	123.73	8.45	123.57	8.37	123.24
70	9.09	125.37	8.51	122.59	8.45	122.21
71	8.17	122.46	8.55	126.59	8.49	125.96
72	8.53	123.42	8.56	122.90	8.54	122.65
73	8.41	124.68	8.57	124.01	8.53	123.62
74	8.50	122.13	8.61	121.77	8.54	121.65
75	8.54	111.18	8.18	110.80	8.53	110.63
76	7.97	114.84	0.20	115.21	8.17	115.15

Table S2: Proline isomerization rates, k_{ex}, at different temperature and pressures, and corresponding Arrhenius activation energies, EA, for two synthetic peptides.

	k_{ex} (s^{-1}) 323 K	k_{ex} (s^{-1}) 327 K	k_{ex} (s^{-1}) 330 K	k_{ex} (s^{-1}) 333 K	E_A (kcal.mol^{-1})
acetyl-EVEPSDT-NH_2, 1bar	0.40 ± 0.06	0.60± 0.09	0.8 ± 0.1	1.1 ± 0.1	21.4 ± 3.9
acetyl-EVEPSDT-NH_2, 2.5kbar	0.25± 0.03	0.36 ± 0.04	0.49 ± 0.07	0.65 ± 0.06	20.3 ± 3.3
acetyl-EVFPSDT, 1bar	0.41 ± 0.04	0.57 ± 0.06	0.79 ± 0.09	1.0 ± 0.1	19.8 ± 3.1
acetyl-EVFPSDT, 2.5 kbar	0.25 ± 0.02	0.36 ± 0.03	0.48 ± 0.03	0.61 ± 0.06	18.9 ± 2.6

References

1. Hartel, A. J.; Lankhorst, P. P.; Altona, C., Nucleic-acid constituents. 24. Thermodynamics of stacking and of self-association of the dinucleoside monophosphate M26A-U from proton NMR chemical shifts-differential concentration temperature profile method. *Eur. J. Biochem.* **1982,** *129* (2), 343-357.
2. Ying, J.; Roche, J.; Bax, A., Homonuclear decoupling for enhancing resolution and sensitivity in NOE and RDC measurements of peptides and proteins. *J. Magn. Reson.* **2014,** *241*, 97-102.
3. Miloushev, V. Z.; Bahna, F.; Ciatto, C.; Ahlsen, G.; Honig, B.; Shapiro, L.; Palmer, A. G., Dynamic properties of a type II cadherin adhesive domain: Implications for the mechanism of strand-swapping of classical cadherins. *Structure* **2008,** *16* (8), 1195-1205.